nature geoscience

LETTERS

PUBLISHED ONLINE: 1 DECEMBER 2013 | DOI: 10.1038/NGEO2019

Delamination and recycling of Archaean crust caused by gravitational instabilities

Tim E. Johnson[1]*, Michael Brown[2], Boris J. P. Kaus[1,3] and Jill A. VanTongeren[4]

Mantle temperatures during the Archaean eon were higher than today. As a consequence, the primary crust formed at the time is thought to have been extensive, thick and magnesium rich, and underlain by a highly residual mantle[1]. However, the preserved volume of this crust today is low, implying that much of it was recycled back into the mantle[2]. Furthermore, Archaean crust exposed today is composed mostly of tonalite–trondhjemite–granodiorite, indicative of a hydrated, low-magnesium basalt source[3], suggesting that they were not directly generated from a magnesium-rich primary crust. Here we present thermodynamic calculations that indicate that the stable mineral assemblages expected to form at the base of a 45-km-thick, fully hydrated and anhydrous magnesium-rich crust are denser than the underlying, complementary residual mantle. We use two-dimensional geodynamic models to show that the base of magmatically over-thickened magnesium-rich crust, whether fully hydrated or anhydrous, would have been gravitationally unstable at mantle temperatures greater than 1,500–1,550 °C. The dense crust would drip down into the mantle, generating a return flow of asthenospheric mantle that melts to create more primary crust. Continued melting of over-thickened and dripping magnesium-rich crust, combined with fractionation of primary magmas, may have produced the hydrated magnesium-poor basalts necessary to source tonalite–trondhjemite–granodiorite melts. The residues of these processes, with an ultramafic composition, must now reside in the mantle.

Understanding the formation and reworking of Earth's early crust is important for models of mantle evolution. Earth's primary crust is a product of partial melting of the mantle. Most primary (oceanic) crust on modern Earth is produced at spreading ridges, is on average 6–7 km thick and is composed of mid-ocean ridge basalts (MORBs; 5–8 wt% MgO), the result of partial melting at melt fractions (F) of 0.08–0.1 and mantle potential temperatures (T_p) of 1,280–1,400 °C (ref. 4). This crust is recycled by subduction during which it is converted to eclogite. On the early Earth things were undoubtedly different. The occurrence of voluminous tonalite–trondhjemite–granodiorite (TTG) crust and komatiites, which are largely restricted to the Archaean[5], and the volume of continental crust produced during the Archaean[6] are consistent with a hotter Earth. Although the thermal evolution of Earth and the mechanism of heat loss remain matters of debate[7,8], higher T_p during the Archaean would have led to more extensive melting of the mantle and production of a thick (up to 45 km) MgO-rich primary crust[1,2]. Komatiite magmatism associated with plumes and excess T_p may have contributed to the early crust, but the volume of komatiite in greenstone belts (0–20 vol%) suggests that this played only a minor role[9].

On the basis of the petrology and geochemistry of volcanic rocks, the composition of model primary melts generated by varying degrees of partial melting of fertile peridotite can be calculated with reference to experiments[4], from which the composition of the complementary residues are constrained by mass balance[1,2]. Near-pristine xenoliths of harzburgite that sample the Archaean lithospheric mantle are highly depleted in FeO, Al_2O_3 and CaO relative to fertile mantle and have compositions that correspond well with modelled residua for melt fractions of 0.25–0.45 and primary crust 25–45 km in thickness[2]. Samples of high-MgO non-arc basalts from Archaean greenstone belts have compositions consistent with their derivation from primary melts[1] (Fig. 1). However, the volume of these rocks in the exposed geologic record is low. Assuming these non-arc basalts are representative of primary crust[1,2], then most of this crust is missing, which suggests that it has been recycled or sequestered at depth in the mantle.

A plot of MgO content versus age for non-arc basalts[1] shows that ambient T_p was >1,500 °C during the Archaean, with a maximum in the Mesoarchaean (Fig. 1a). The inferred onset of secular cooling of the mantle broadly coincides with a marked decrease in the rate of crustal growth around 3 billion years ago[6] (Ga), and may record the transition to dominantly subduction-driven plate tectonics on Earth[10,11]. Before this, most primary crust may have formed by intra- and over-accretion of melts above upwelling mantle driven by smaller wavelength convection[11]. With a higher basal heat flux and increased radiogenic heat production, temperatures close to the base of thick primary crust in the Archaean may have exceeded 1,000 °C (ref. 10), conditions under which partial melting of ultramafic rocks is likely if they were hydrated[12,13].

The range in T_p for any given age suggested by the petrological data (Fig. 1a) is similar to temperature variations in mantle upwelling beneath modern mid-ocean ridges[4], and would have given rise to variations in the composition and thickness of Archaean primary crust (Fig. 1c) and associated residual mantle. Such variations may have allowed different tectonic styles to operate in different parts of the ancient Earth[11]. Extreme ambient mantle temperatures (T_p > 1,600 °C) could have produced *in situ* primary crust 40–45 km thick[2] (Fig. 1c). Subduction similar to that observed in contemporary plate tectonics may not have been possible under these conditions[8,11,14].

Here we test the postulate that thick primary crust produced in the early Archaean could have become gravitationally unstable

[1]Institute for Geoscience, University of Mainz, Mainz 55099, Germany, [2]Department of Geology, University of Maryland, College Park, Maryland 20742, USA, [3]Department of Earth Sciences, University of Southern California, Los Angeles, California 90089-0740, USA, [4]Department of Geology & Geophysics, Yale University, New Haven, Connecticut 06511, USA. *e-mail: tjohnson@uni-mainz.de

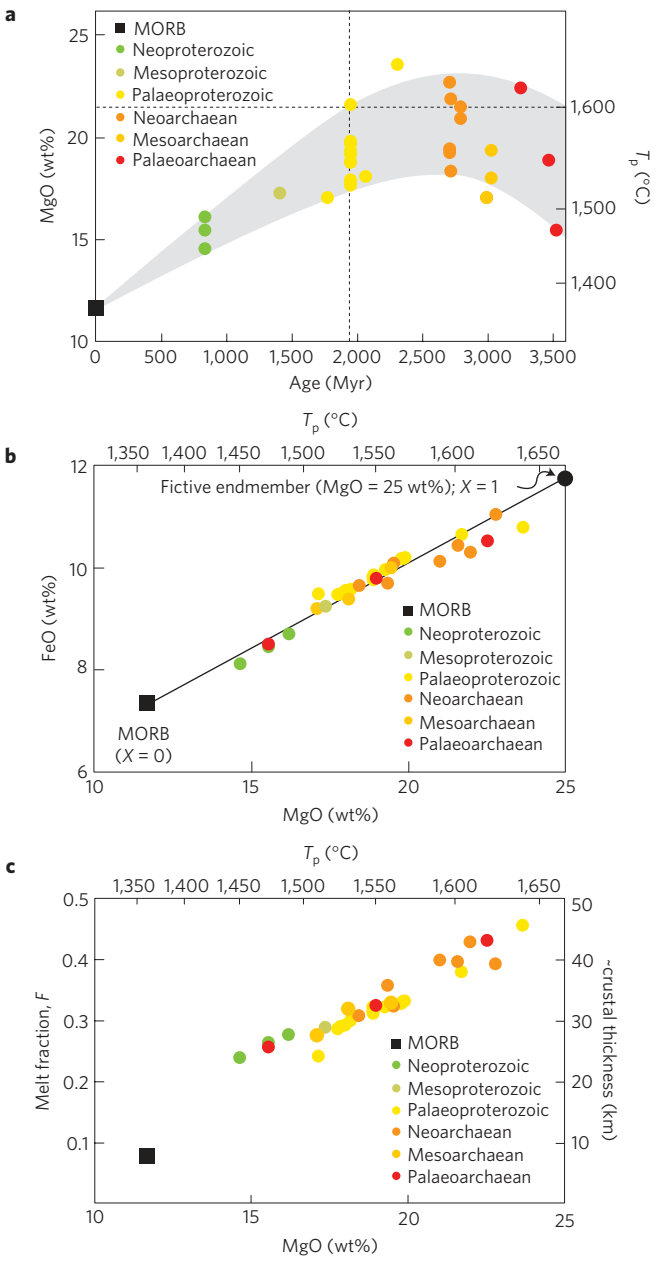

Figure 1 | Calculated primary melt compositions for Precambrian non-arc basalts. a, MgO (mantle potential temperature) versus age (see Supplementary Information for Fig. 1a); ambient mantle potential temperature peaked during the Archaean. **b**, MgO (mantle potential temperature) versus FeO; the primary melt compositions for MORB ($X = 0$) and a fictive composition with 25 wt% MgO ($X = 1$) define endmembers of the binary compositional range used in the thermodynamic modelling. **c**, MgO (mantle potential temperature) versus melt fraction (F) based on the relationship $F = 1.456–2.189$ (FeO/MgO); ~1 km of crust is produced per 1 vol% melting[2].

with respect to the underlying mantle residues so that if locally thickened it became negatively buoyant and could have delaminated by Rayleigh–Taylor instabilities. To do this we model the equilibrium (minimum Gibbs free energy) mineral assemblages developed near the base of the crust for a wide range of metamorphosed (hydrated and anhydrous) primary crust compositions (Fig. 2a,b and Supplementary Figs 1–4) and their complementary (anhydrous) residues (Fig. 2c and Supplementary Figs 5 and 6) that account for secular changes in T_p, F and crustal thickness (Methods). First, we calculate the stability of equilibrium mineral assemblages for a temperature of 1,000 °C (Fig. 2a,b and Supplementary Figs 1 and 3), which corresponds to that expected near the base of 30–45-km-thick crust based on the apparent thermal gradients recorded by Mesoarchaean to Neoarchaean metamorphic rocks[10] and approximates the solidus temperature of hydrated ultramafic primary crust, inferred to lie between the fluid-absent solidi for amphibolite and amphibole-bearing MORB pyrolite and wehrlite[13,15]. To assess the temperature sensitivity of the results, we also calculate phase equilibria at 900 °C (Fig. 2a and Supplementary Figs 2 and 4). We use the results to calculate the density (ρ) contrast at the crust–mantle interface for the range of compositions and temperatures modelled to assess the stability of the crust relative to the underlying residual mantle (Fig. 3). We incorporate the density data with a parameterized melting and melt extraction algorithm into a two-dimensional (2D) thermomechanical model (Methods) to evaluate the dynamical plausibility of crustal recycling by Rayleigh–Taylor instabilities for endmember simulations involving either hydrated or anhydrous crust (Supplementary Section 3), wet or dry mantle, and various crustal thicknesses, T_p and Moho temperatures (Fig. 4 and Supplementary Figs 8–12). By integrating results from both thermodynamic and 2D numerical modelling, we draw several important inferences about Archaean tectonics, partial melting of delaminated primary crust, intracrustal differentiation and the generation of TTG magmas.

The variation in density between fully hydrated and anhydrous crust is shown in Fig. 3a,b, the density of the complementary residual mantle in Fig. 3c, and the effect on the potential instability of the crust in Fig. 3d. Thick anhydrous crust and hydrated primary crust with high MgO (>21–22 wt%), generated at extreme T_p (>1,600 °C), would have been gravitationally unstable at its base (Fig. 3d). Primary melts with lower MgO (< or ≪21 wt%; T_p < 1,600 °C) would have produced lower crustal thicknesses (Fig. 1c) and over-thickening would be required for the base to become gravitationally unstable (Fig. 3d).

Here we illustrate the results of the geodynamic modelling with reference to one experiment for the evolution of primary crust during the early Archaean (Fig. 4). Thick MgO-rich primary crust forms above hot upwelling mantle by near-isentropic melting. Local thickening causes material at the base of the crust to become gravitationally unstable. Using 2D thermomechanical modelling we are able to show that delamination of this over-thickened primary crust occurs by Rayleigh–Taylor instabilities once the viscosity is sufficiently low (Fig. 4) and occurs for a range of crustal thicknesses and geotherms (Methods and Supplementary Information, 3 Geodynamic numerical modelling). A scaling analysis reveals that the two requirements for the instabilities to occur are a sufficiently thick negatively buoyant lower crust and low effective viscosities of the uppermost mantle and lower crust (see Supplementary Information 3.2.3). For realistic rheologies, this mechanism starts to operate at $T_p = 1,500–1,550$ °C but is particularly effective at $T_p \geq 1,600$ °C, consistent with predicted upper mantle temperatures in the Archaean (Fig. 1). Sinking primary crust could have partially melted directly to produce basalt[16] and/or reacted with and refertilized the underlying residual mantle to induce further melting[16,17]. Mantle return flow would have caused additional adiabatic melting and further crustal thickening (Fig. 4 and Supplementary Section 3). At the predicted temperatures, partial melting near the base of over-thickened hydrated primary crust would result in intracrustal differentiation. These secondary magmas would have had lower MgO contents than the primary crust.

The depths at which the base of the primary crust becomes gravitationally unstable represent maxima. First, the modelled

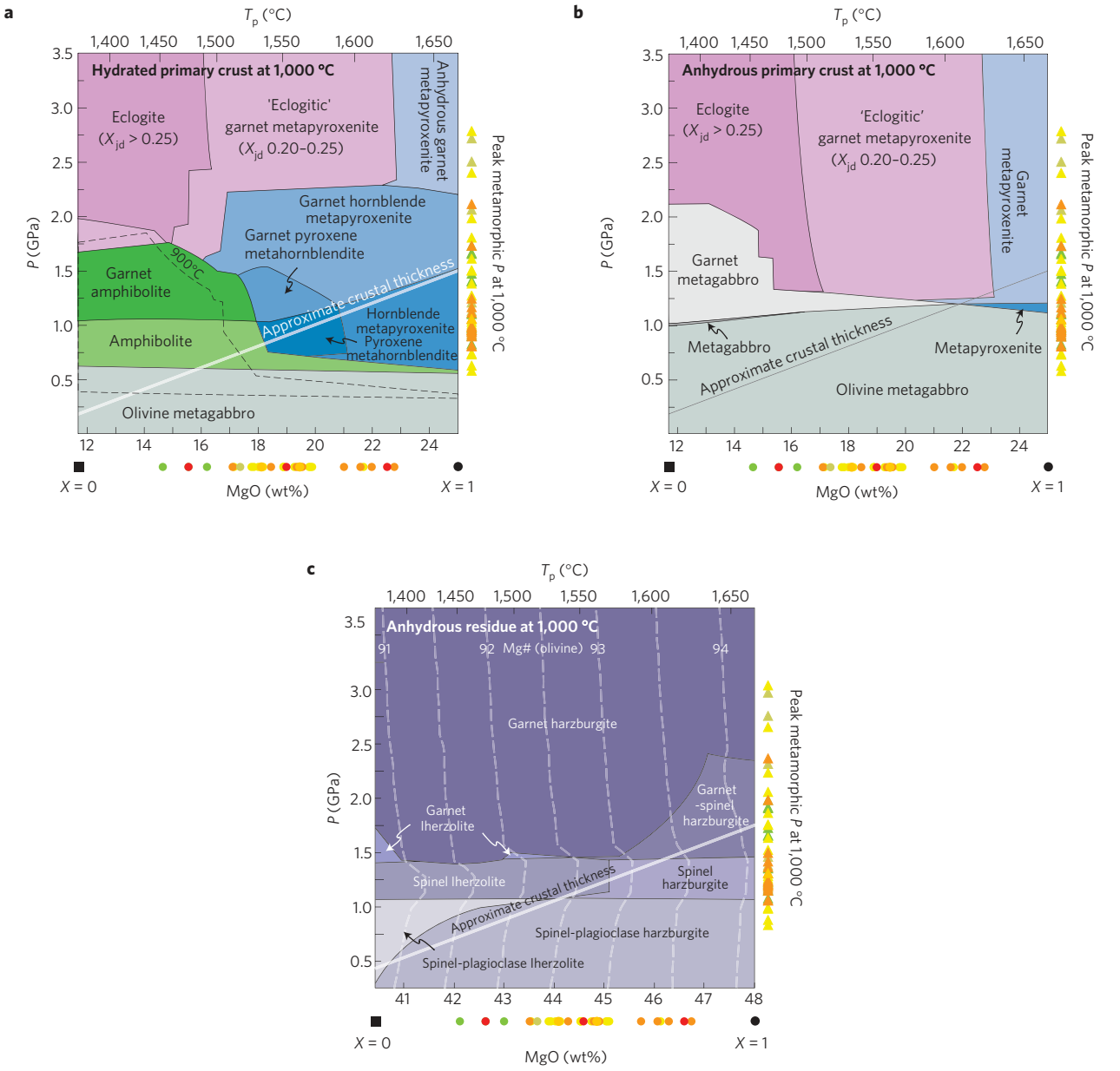

Figure 2 | Results of thermodynamic modelling of primary crust and complementary residues at 1,000 °C. a–c, Metamorphic rock types based on mineral assemblage stability fields for hydrated (**a**) and anhydrous (**b**) primary crust, and complementary residues (**c**; see Supplementary Figs 1–6; in **a**, note reduced stability field for amphibolite at 900 °C); line shows approximate thickness of primary crust in relation to MgO content. Primary melt compositions for Precambrian non-arc basalts and inferred mantle potential temperatures (T_p) are shown along the abscissa. Extrapolated pressures at 1,000 °C (right-hand ordinate) are based on apparent thermal gradients recorded by metamorphosed Precambrian rocks[10].

crust is taken to be homogeneous. However, similar to present-day primary crust (intra-oceanic arc crust[18], oceanic plateaux[19,20] and oceanic crust[21]), primary crust in the Archaean is likely to have differentiated into lower-MgO and higher-MgO (cumulate-rich) portions[19]. Second, the modelled residua (Fig. 2c) are the average compositions of the melt-depleted mantle and do not account for the decrease in the degree of partial melting with depth. Consequently, the residual mantle immediately underlying the crust would have been more depleted, and marginally less dense, than modelled.

We emphasize that high-MgO (> or ≫18 wt% MgO) primary crust produced during the Archaean would have been ultramafic not basaltic[14]. Compositions in the lower portion of over-thickened primary crust would have been silica-undersaturated metapyroxenite or metahornblendite, additionally containing garnet at higher pressures (>1.0–1.5 GPa) or at lower degrees of hydration (Fig. 2a,b and Supplementary Figs 1 and 3). High-MgO garnet metapyroxenite (16–23 wt% MgO) xenoliths of Archaean age have mantle-like oxygen isotopic compositions[22–24] and generally record high equilibrium temperatures[22]. They are compositionally and mineralogically similar to modelled high-MgO compositions[22] and may represent near-pristine primary crust that foundered into the depleted mantle[24]. In contrast, low-MgO eclogite xenoliths have omphacitic clinopyroxene, highly variable oxygen isotopic compositions and may contain accessory kyanite, quartz/coesite, K-feldspar and/or corundum[23]. They probably represent highly fractionated crustal compositions with a multi-stage evolutionary history[22].

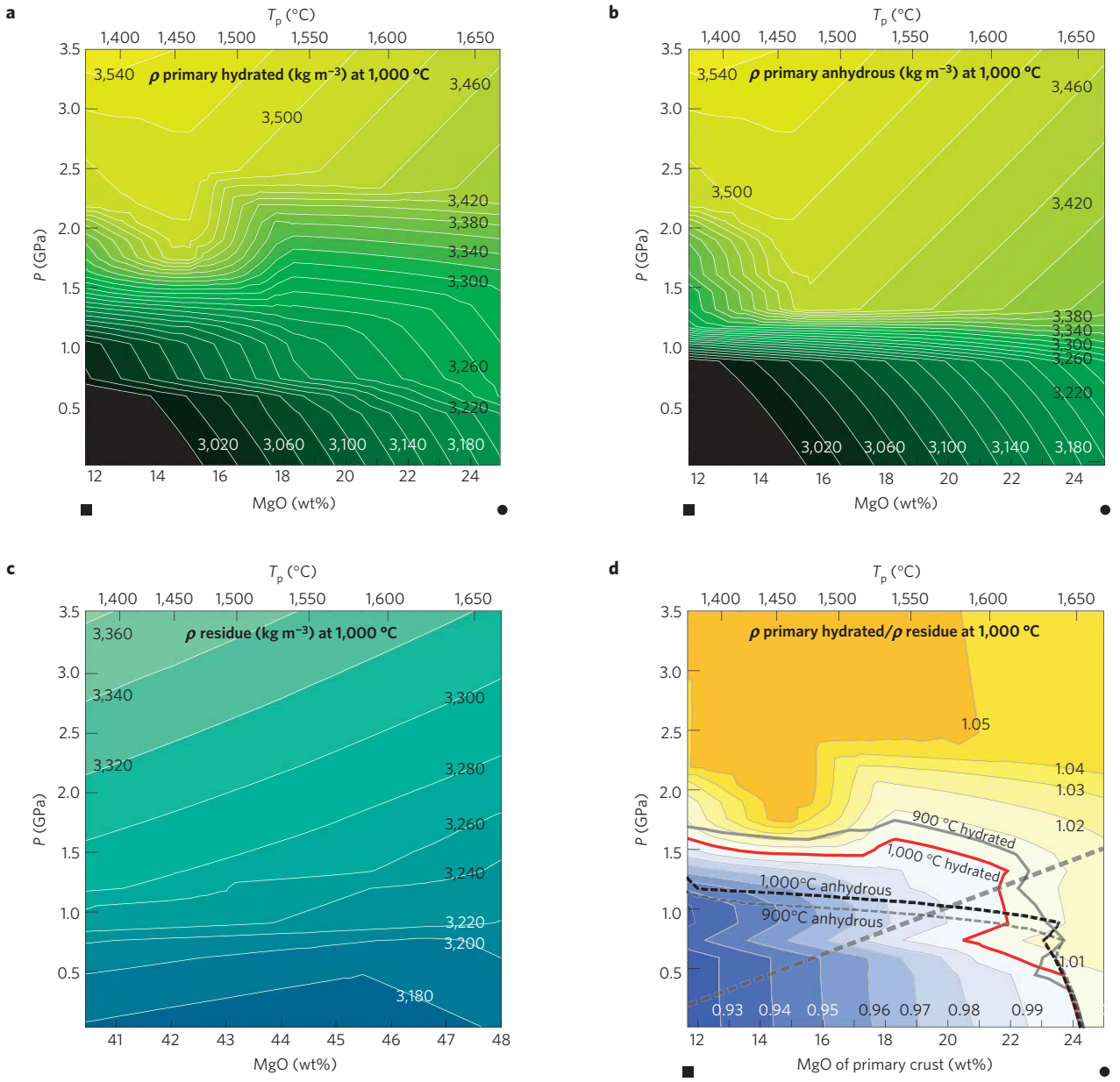

Figure 3 | Density (ρ) of primary crust and complementary residues. a–c, Densities calculated at 1,000 °C plotted against MgO content for hydrated primary crust (**a**), anhydrous primary crust (**b**) and the complementary residues (**c**). **d**, The relative density of hydrated crust compared with the underlying residual mantle at 1,000 °C against MgO of the primary crust with the equality line for anhydrous crust at 1,000 °C and those for 900°C (based on Supplementary Fig. 7) superimposed. The solid (hydrated) and dashed (anhydrous) lines separate stable primary crust (below) from potentially unstable primary crust (above).

The high SiO_2, Na/K and Sr/Y and depleted heavy rare earth element contents of sodic Archaean TTGs suggest that most were derived by partial melting of garnet amphibolite[3,25]. At 1,000 °C garnet amphibolite is stable only in hydrated primary crust with MgO < or ≪18 wt% at P > 1.0 GPa (Fig. 2a and Supplementary Fig. 1), and this stability is further reduced at 900 °C (Fig. 2a and Supplementary Fig. 3). Thus, TTG melts cannot have been generated from partial melting of unmodified Archaean high-MgO primary crust, which would result in basaltic or nephelinitic melt compositions[14], but were derived from crust of basaltic composition[3]. This basaltic crust could have been produced by differentiation of primary melts by crystal fractionation[14] or by partial melting of over-thickened primary crust. Thus, a two-stage process is required for the production of Archaean TTG magmas.

Although the thermal structure of the mantle in the Hadean and Eoarchaean is poorly constrained, primary crustal compositions indicating T_p > 1,600 °C seem to be limited to occurrences between around 3.5 Ga (or earlier) and around 1.9 Ga (Fig. 1a). This interval spans the onset of production of ultrathick primary crust and tectonics dominated by Rayleigh–Taylor instabilities to the transition to a dominantly modern-style of subduction, and may define an early tectonic regime with globally variable tectonic styles controlled by the spatial range in T_p at any point in time[11]. Rather than subduction-driven plate tectonics, delamination by Rayleigh–Taylor instabilities of over-thickened primary crust was responsible for the production and stabilization of the bulk of the continental crust.

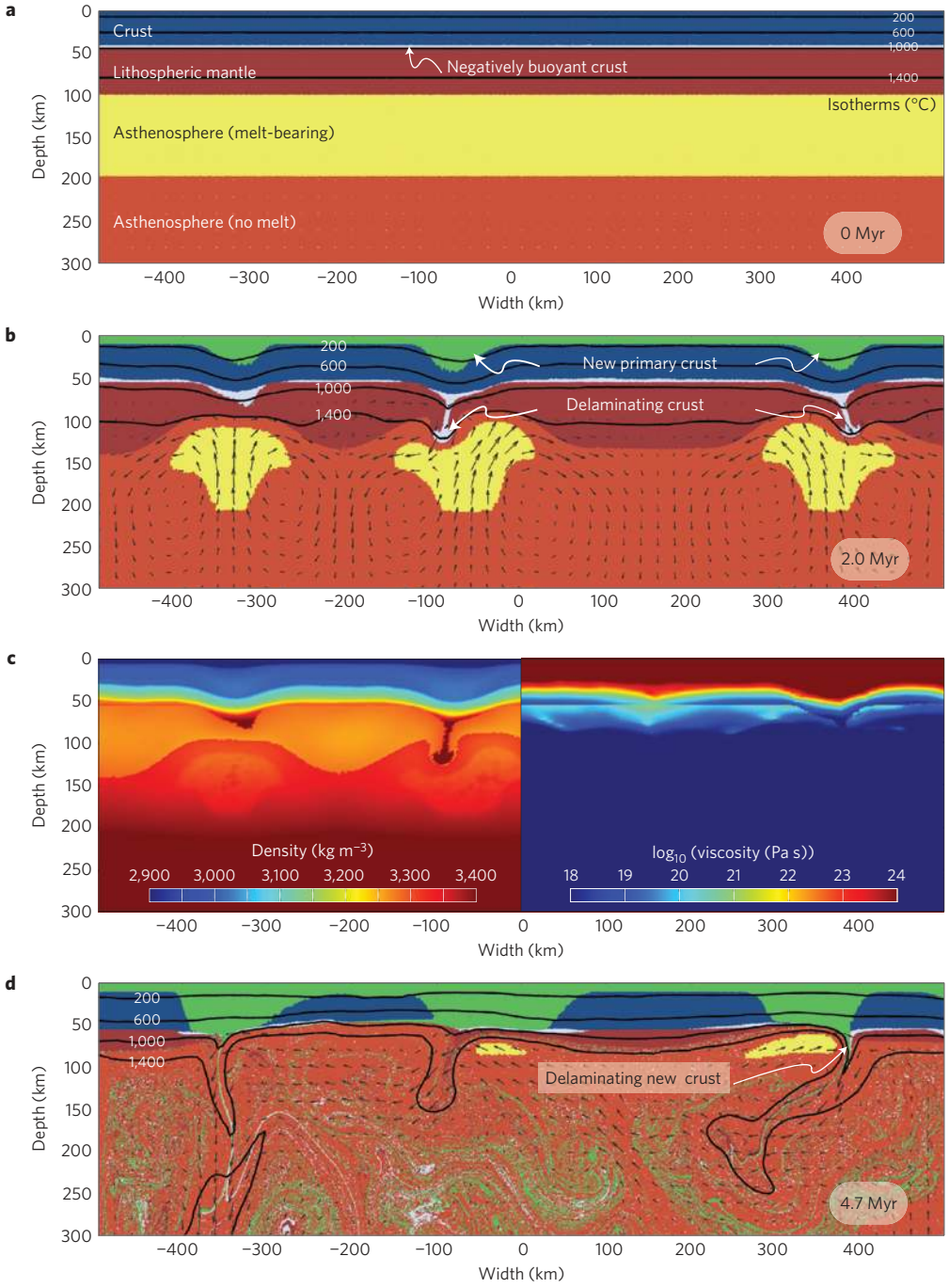

Figure 4 | Results of geodynamic modelling; snapshots from an experiment with 45-km-thick initial primary crust and T_p of 1,600 °C. a, Model configuration and initial conditions (dark blue, initial primary crust; light blue, negatively buoyant initial primary crust; red, lithospheric mantle; orange, unmelted asthenosphere; yellow, melt-bearing asthenosphere). **b**, Local thickening of the initial primary crust by addition of new primary crust (green) and delamination of negatively buoyant initial primary crust. Large-scale mantle flow is caused mainly by the positive buoyancy of the melt-bearing asthenosphere; crustal drips induce smaller circulation patterns. **c**, Density (left) and viscosity (right) for the left-hand and right-hand halves of **b**, respectively. **d**, Local thickening and delamination of negatively buoyant new primary crust.

Methods

The phase equilibria are presented as isothermal pressure (P)–composition (X) pseudosections calculated in the chemical systems Na_2O–CaO–FeO–MgO–Al_2O_3–SiO_2–H_2O–TiO_2–O_2 for the primary melt compositions (Supplementary Figs 1, 3, 7 and 9) and CaO–FeO–MgO–Al_2O_3–SiO_2–O_2 for the complementary residue compositions (Supplementary Figs 5 and 11) using Perple_X (ref. 26) with internally consistent thermodynamic data for endmembers[27] and the most recently calibrated activity–composition models for solid-solution phases[28] (see Supplementary Section 2). The modelled compositional range for primary crust is a binary mixture between the primary melt composition for MORB ($X = 0$) and a fictive endmember composition (MgO of 25 wt%; $X = 1$) as a proxy for primary crust generated at extreme T_p (Fig. 1). The composition (in mol%) of these endmembers in terms of the components SiO_2, TiO_2, Al_2O_3, FeO, MgO, CaO, Na_2O, O_2 is: 49.49, 0.66, 10.11, 6.69, 17.72, 12.72, 2.28, 0.33 ($X = 0$) and 42.96, 0.60, 2.61, 10.09, 34.97, 7.53, 0.99, 0.25 ($X = 1$). The endmember compositions of the binary bulk compositional range for the complementary residue in terms of the components SiO_2, Al_2O_3, FeO, MgO, CaO, O_2 are: 38.25, 1.61, 5.80, 51.66, 2.53, 0.15 ($X = 0$) and 35.76,

1.28, 4.07, 58.52, 0.27, 0.10 ($X = 1$). All calculations use a $Fe^{3+}/(Fe^{3+} + Fe^{2+})$ ratio of 0.1 (see Supplementary Section 2). The phase equilibria modelling considers the phases olivine, garnet, clinopyroxene, orthpyroxene, hornblende, plagioclase, quartz, ilmenite, rutile, spinel, magnetite, haematite and H_2O. On the basis of the phase equilibria, densities are calculated for hydrated primary crust, anhydrous primary crust and the complementary residues to determine the relative densities of hydrated or anhydrous crust compared with the underlying residual mantle at 1,000 and 900 °C.

The parameterized 2D thermomechanical models solve the governing conservation equations of mass, momentum and energy of slowly creeping fluids on geological timescales using the finite element code MILAMIN_VEP (refs 29,30). The code employs realistic rock densities that have been computed as a function of P and T for the given rock types described above, as well as laboratory-constrained creep laws. In addition, we have implemented partial melting of mantle lithosphere and underlying fertile mantle, and added a simplified melt extraction algorithm that removes melt from the mantle as soon as >5% melt is present and emplaces it on top of the crust. We have performed systematic studies to understand the sensitivity of the results to input parameters, and developed a scaling analysis that demonstrates that the underlying physics of the models is governed by density-driven instabilities that erode the base of the crust in relatively small pulses once the viscosity of the mantle lithosphere underneath the crust is sufficiently low (see Supplementary Section 3).

Received 20 March 2013; accepted 29 October 2013; published online 1 December 2013

References

1. Herzberg, C., Condie, K. & Korenaga, J. Thermal history of the Earth and its petrological expression. *Earth Planet. Sci. Lett.* **292,** 79–88 (2010).
2. Herzberg, C. & Rudnick, R. Formation of cratonic lithosphere: An integrated thermal and petrological model. *Lithos* **149,** 4–15 (2012).
3. Foley, S., Tiepolo, M. & Vannucci, R. Growth of early continental crust controlled by melting of amphibolite in subduction zones. *Nature* **417,** 837–840 (2002).
4. Herzberg, C. *et al.* Temperatures in ambient mantle and plumes: Constraints from basalts, picrites and komatiites. *Geochem. Geophys. Geosyst.* **8,** Q02006 (2007).
5. Goodwin, A. *Precambrian Geology: The Dynamic Evolution of the Continental Crust* (Academic, 1991).
6. Dhuime, B., Hawkesworth, C. J., Cawood, P. A. & Storey, C. D. A change in the geodynamics of continental growth 3 billion years ago. *Science* **335,** 1334–1336 (2012).
7. Davies, G. F. Effect of plate bending on the Urey ratio and the thermal evolution of the mantle. *Earth Planet. Sci. Lett.* **287,** 513–518 (2009).
8. Van Hunen, J. & Moyen, J-F. Archean subduction: Fact or fiction? *Annu. Rev. Earth Planet. Sci.* **40,** 195–219 (2012).
9. Arndt, N. T. & Lesher, C. M. in *Komatiites* (eds Selley, R. C., Cocks, L. R. M. & Plimer, I. R.) 260–267 (Encyclopedia of Geol., Vol. 3, Elsevier, 2005).
10. Brown, M. Metamorphic conditions in orogenic belts: A record of secular change. *Int. Geol. Rev.* **49,** 193–234 (2007).
11. Sizova, E., Gerya, T., Brown, M. & Perchuk, L. Subduction styles in the Precambrian: Insight from numerical experiments. *Lithos* **116,** 209–229 (2010).
12. Mareschal, J-C. & Jaupart, C. 61–73 (Geophys. Monogr. Ser., Vol. 164, AGU, 2006).
13. Niida, K. & Green, D. H. Stability and chemical composition of pargasitic amphibole in MORB pyrolite under upper mantle conditions. *Contrib. Mineral. Petrol.* **135,** 18–40 (1999).
14. Foley, S. F., Buhre, S. & Jacob, D. E. Evolution of the Archaean crust by delamination and shallow subduction. *Nature* **421,** 249–252 (2003).
15. Rushmer, T. Partial melting of two amphibolites: Contrasting experimental results under fluid-absent conditions. *Contrib. Mineral. Petrol.* **107,** 41–59 (1991).
16. Elkins-Tanton, L. T. Continental magmatism, volatile recycling, and a heterogeneous mantle caused by lithospheric gravitational instabilities. *J. Geophys. Res.* **112,** B03405 (2007).
17. Bedard, J. H. A catalytic delamination-driven model for coupled genesis of Archaean crust and sub-continental lithospheric mantle. *Geochim. Cosmochim. Acta* **70,** 1188–1214 (2006).
18. Jagoutz, O., Müntener, O., Schmidt, M. W. & Burg, J-P. The roles of flux- and decompression melting and their respective fractionation lines for continental crust formation: Evidence from the Kohistan arc. *Earth Planet. Sci. Lett.* **303,** 25–36 (2011).
19. Kerr, A. C., Tarney, J., Nivia, A., Marriner, G. F. & Saunders, A. D. The internal structure of oceanic plateaus: Inferences from obducted Cretaceous terranes in western Colombia and the Caribbean. *Tectonophysics* **292,** 173–188 (1998).
20. Fitton, J. G., Mahoney, J. J., Wallace, P. J. & Saunders, A. D. (eds) Origin and evolution of the ontong Java plateau. *Geol. Soc. Spec. Publ.* **229,** 1–368 (2004).
21. Kelemen, P. B., Koga, K. & Shimizu, N. Geochemistry of gabbro sills in the crust-mantle transition zone of the Oman ophiolite: Implications for the origin of the oceanic lower crust. *Earth Planet. Sci. Lett.* **146,** 475–488 (1997).
22. Gonzaga, R. *et al.* Eclogites and garnet pyroxenites: Similarities and differences. *J. Volcanol. Geotherm. Res.* **190,** 235–247 (2010).
23. Jacob, D. Nature and origin of eclogite xenoliths from kimberlites. *Lithos* **77,** 295–316 (2004).
24. Barth, M. G. *et al.* Geochemistry of xenolithic eclogites from West Africa, part 2: Origins of the high MgO eclogites. *Geochim. Cosmochim. Acta* **66,** 4325–4345 (2002).
25. Moyen, J-F. The composite Archaean grey gneisses: Petrological significance, and evidence for a non-unique tectonic setting for Archaean crustal growth. *Lithos* **123,** 21–36 (2011).
26. Connolly, J. A. D. Computation of phase equilibria by linear programming: A tool for geodynamic modeling and its application to subduction zone decarbonation. *Earth Planet. Sci. Lett.* **236,** 524–541 (2005).
27. Holland, T. J. B. & Powell, R. An internally consistent thermodynamic data set for phases of petrological interest. *J. Metamorph. Geol.* **16,** 309–343 (1998).
28. Diener, J. F. A. & Powell, R. Revised activity-composition relations for clinopyroxene and amphibole. *J. Metamorph. Geol.* **30,** 131–142 (2012).
29. Thielmann, M. & Kaus, B. Shear heating induced lithospheric-scale localization: Does it result in subduction? *Earth Planet. Sci. Lett.* **359-360,** 1–13 (2012).
30. Kaus, B. Factors that control the angle of shear bands in geodynamic numerical models of brittle deformation. *Tectonophysics* **484,** 36–47 (2010).

Acknowledgements

We thank S. Aulbach, J. Connolly, G. Davies, S. Fischer, S. F. Foley, E. C. R. Green, C. Herzberg, D. E. Jacob and R. W. White for comments. M.B. and T.E.J. acknowledge financial support from the Geocycles Earth Systems Research Centre, University of Mainz. B.J.P.K. was financially supported by ERC Starting Grant 258830.

Author contributions

M.B. and T.E.J. developed the project; T.E.J. calculated the phase diagrams and B.J.P.K. developed and ran the numerical models. All authors discussed the results and were involved in writing the paper.

Additional information

Supplementary information is available in the online version of the paper. Reprints and permissions information is available online at www.nature.com/reprints. Correspondence and requests for materials should be addressed to T.E.J.

Competing financial interests

The authors declare no competing financial interests.